HHS Public Access

Author manuscript

Cancer Lett. Author manuscript; available in PMC 2018 November 28.

Published in final edited form as:

Cancer Lett. 2017 November 28; 409: 30–41. doi:10.1016/j.canlet.2017.08.019.

PAD1 promotes epithelial-mesenchymal transition and metastasis in triple-negative breast cancer cells by regulating MEK1-ERK1/2-MMP2 signaling

Hao Qin[1,#], **Xiaoqiu Liu**[2,#], **Fujun Li**[1], **Lixia Miao**[1], **Tingting Li**[1], **Boqun Xu**[3], **Xiaofei An**[4], **Aaron Muth**[5], **Paul R Thompson**[5], **Scott A Coonrod**[6], and **Xuesen Zhang**[1,*]

[1]State Key Laboratory of Reproductive Medicine, Nanjing Medical University, Nanjing, 211166, China

[2]Department of Microbiology, Key Laboratory of Pathogen Biology of Jiangsu Province, Nanjing Medical University, Nanjing, 211166, China

[3]Department of Obstetrics and Gynecology, The Second Affiliated Hospital of Nanjing Medical University, Nanjing, 210000, China

[4]Department of Endocrinology, Jiangsu Province Hospital of Chinese Medicine, The Affiliated Hospital of Nanjing University of Chinese Medicine, Nanjing, 210029, China

[5]Department of Biochemistry and Molecular Pharmacology, University of Massachusetts Medical School, Worcester, MA, 01655, USA

[6]Baker Institute for Animal Health, College of Veterinary Medicine, Cornell University, New York, 14853, USA

Abstract

Peptidylargininedeiminase 1 (PAD1) catalyzes protein for citrullination, and this activity has been linked to the epidermal cornification. However, a role for PAD1 in tumorigenesis, including breast cancers has not been previously explored. Here we first showed that PAD1 is overexpressed in human triple negative breast cancer (TNBC). In cultured cells and xenograft mouse models, PAD1 depletion or inhibition reduced cell proliferation, suppressed epithelial-mesenchymal transition, and prevented metastasis of MDA-MB-231 cells. These changes were correlated with a dramatic decrease in MMP2/9 expression. Furthermore, ERK1/2 and P38 MAPK signaling pathways are activated upon PAD1 silencing. Treatment with MEK1/2 inhibitor in PAD1 knockdown cells significantly recovered MMP2 expression, while inhibiting P38 activation only slightly elevated MMP9 levels. We then showed that PAD1 interacts with and citrullinates MEK1 thereby disrupting MEK1-catalyzed ERK1/2 phosphorylation, thus leading to the MMP2 overexpression. Collectively, our data indicate that PAD1 appears to promote tumorigenesis by regulating MEK1-ERK1/2-MMP2 signaling in TNBC. These results also raise the possibility that PAD1 may

[*]**Corresponding Author:** Xuesen Zhang, State Key Laboratory of Reproductive Medicine, Nanjing Medical University, Nanjing, China, 211166. Phone: 86-25-86869510; Fax: 86-25-86869510; xuesenzhang@njmu.edu.cn.
[#]These authors contribute equally to this work.

Conflict of interest statement

The authors declare that there are no conflicts of interest.

function as an important new biomarker for TNBC tumors and suggest that PAD1-specific inhibitors could potentially be utilized to treat metastatic breast cancer.

Keywords

PAD1; triple-negative breast cancer; metastasis; MEK/ERK; MMP2

1. Introduction

The triple-negative breast cancer (TNBC) refers to the breast cancer tested negative for estrogen receptor (ER), progesterone receptor (PR) and human epidermal growth factor receptor 2 (HER2), and it is the most invasive and aggressive among the breast cancer subtypes. Management of TNBC is particularly challenging due to the lack of effective therapeutic targets, aggressive cell behavior, and relatively poor prognosis [1,2]. Therefore, elucidation of the molecular events responsible for the regulation of invasion and metastasis of TNBC may aid in identifying the new targets for an improved diagnosis and treatment of patients with metastatic TNBC.

Metastasis of cancer cells occurs through a complex series of events involving loss of cell-cell adhesion, migration, invasion, unrestrained cell proliferation and angiogenesis [3,4]. One of the first steps of metastasis is the degradation of the basement membrane and stromal extracellular matrix (ECM), which form physical barriers to restrict cell movement [5,6]. During this process, matrix metalloproteinases (MMPs) are involved in the breakdown of the ECM components, thereby facilitating tumor progression and metastasis [4,7,8]. Among them, both MMP2 and MMP9 have been extensively studied. Overexpression of these factors is observed in malignant tumors and positively correlates with an aggressive malignant phenotype and poor outcome in breast cancer patients [9,10]. For example, MMP2 has been found to be an important factor for selectively mediating lung metastasis in a mouse model of breast cancer [11] and human breast cancers [12], while MMP9 is a member of the “70-gene classifier” that is able to predict distant metastasis in lymph-node negative breast cancer patients [13]. Therefore, MMP-2 and MMP-9 appear to have clinical value as both diagnostic factors and predictive factors of metastases for breast cancer.

The peptidylarginine deiminase (PAD) family of enzymes post-translationally convert positively charged arginine residues in substrate proteins to the neutral citrulline and this enzymatic activity is referred to citrullination. The PAD gene family consists of five members (PAD1–4, 6) located within a highly organized gene cluster at 1p36.13 in humans and on the orthologous region of mouse chromosome 4 [14,15]. Interestingly, this locus is predicted to contain a novel, yet to be defined, tumorigenesis-related protein [16]. Recently, PAD -mediated protein citrullination has gathered increased attention due to its emerging role in various cancers [17]. For example, PAD2 and PAD4 can catalyze citrullination of histone H3 and H4 at gene promoters, leading to local changes in chromatin structure and modulation of tumor-associated gene transcription in human breast cancer cells [18,19]. PAD4 was also found to mediate citrullination of histone H3 at the apoptosis-related gene promoters in other cancer cells [20,21]. In addition to the citrullination of specific residues

in the N-terminal histone tails, PAD4 also targets non-histone proteins for citrullination, including glycogen synthase kinase-3β [22], Ets-like protein-1 [23], p300 [24], nucleophosmin [25], DNA methyltransferase DNMT3A [26], antithrombin [27,28] and inhibitor of growth 4 [29]. These studies help clarify the critical roles of citrullination in diverse cellular signaling pathways in tumor cells. Furthermore, the observation that overexpression of PAD2 and PAD4 was detected in a wide range of human malignant cancers [17,30–33] and that PAD inhibitors suppress the proliferation of cancer cell lines both *in vitro* and *in vivo* [34,35], supports the hypothesis that PAD2 and PAD4 play important roles in tumorigenesis, potentially through mediating protein arginine citrullination.

While the role of PAD1 in mammalian biology is not well defined, this isozyme has been previously described in the literature as functioning within the epidermis, where it targets the intermediate filaments, keratin and filaggrin for citrullination to promote epidermal cornification [36]. The loss of charge on target substrates following PAD1-mediated citrullination is believed to lead to disassembly of the cytokeratin-filaggrin complex and proteolytic degradation of these targets. Aside from its role in epidermal function, very little is known about potential functions of PAD1 in other physiological or pathological activities. Given the emerging importance of PAD2 and PAD4 in breast carcinoma, in this report, we first tested for associations between PAD1 and breast cancer and then upon finding a connection between PAD1 and TNBC, explored the molecular mechanisms by which PAD1 could mediate TNBC invasion and metastasis using the MDA-MB-231 model system.

2. Materials and methods

2.1. Cell culture

HEK293, MDA-MB-231, MCF-7 and MDA-MB-468 cell lines were maintained in DMEM supplemented 10% fetal bovum serum at 37°C in a humidified 5% CO2 atmosphere. PAD1-depleted MDA-MB-231 cells were generated by transduction with Mission Lentiviral Transduction Particles containing a short hairpin RNA (shRNA) construct targeting the human PAD1 coding sequence (Sigma SHCLND-NM_013358). In the control group, cells were transduced with a non-targeting shRNA lentiviral construct (Sigma SHC002V). Cells were selected by medium containing 1 μg/ml puromycin (Sigma, USA). Cells were selected under 1 μg/ml puromycin. For cell proliferation assay, cells were seeded into 6-cell plates at a density of 40,000 cells per well and assessed by cell counting on day 1, 2, 3, 4, 5, and 6 post cell seeding. Soft agar colony formation assay was performed by using 0.3% agar in complete medium with cells as the feeder layer and 0.6% agar in complete medium as the bottom layer. Where indicated, D-Cl-amidine was diluted in cell culture medium at the final concentration of 100 μM and added to cells for indicated time before harvest. Where indicated, cells were serum starved for 12 hr and subsequently stimulated with U0126 (10 μM), or SB203580 (10 μM) for 4 hr before harvest.

2.2. Immunohistochemistry

Five cases from each group, which represented TNBC or non-TNBC patients, were selected. Normal human breast tissues were used as controls. Sections were deparaffinized,

rehydrated, and then incubated for 10 min in 3% H2O2 to quench endogenous peroxidase activity. Sections were then heated to retrieve the antigen and then blocked with 10% goat serum in PBS. Immunohistochemical analyses were performed using a Histostain Kit (Invitrogen, USA) with antibodies against ERα, PR, HER2 (Abcam, USA), and PAD1 (Sigma, USA) overnight at 4°C. Sections stained were examined using a Zeiss Axio Observer microscope.

2.3. Transwell invasion assay

A Transwell invasion assay was performed in 24-well plates with 8-μm pore size chamber inserts (Corning, USA), according to the protocols recommended by the manufacturer. Briefly, the upper surface of the filter was coated with 50 μL of Matrigel diluted 1:3 in serum-free DMEM. Approximately 4×10^4 cells were added to the upper chamber of Matrigel-coated Transwell plate (Corning) and cultured in serum-free DMEM. The lower compartment of the Transwell chamber was filled with 600 μL complete media. Cells on the lower surface were then fixed with 4% paraformaldehyde, stained with 0.1% crystal violet and photographed in three independent fields for each well under light microscope at a magnification of × 40. They were finally extracted with 33% acetic acid and detected quantitatively using a standard microplate reader (OD at 570 nm).

2.4. Wound-healing assay

Cell migration was assessed using wound-healing assay. Cells were seeded in 6-well plates and grown to full confluence in complete media, with three parallel wells for each condition. The monolayer was scratched with a 10 μL pipette tip, and washed twice with serum-free DMEM to remove the detached cells. The wounded areas were observed and imaged under microscope. The distances were imaged at 0, 3, 6 and 24hr after scratches, respectively. The changes in cell migration were determined by comparing the difference in wound-healing areas at least at 4 fields using ImageJ (National Institute of Mental Health, MA, USA). The data from three independent experiments were used in the calculation of the final data.

2.5. Western blotting

The cells were washed twice with cold PBS and then harvested for Western blotting. Cells were lysed in cold radioimmunoprecipitation assay (RIPA) buffer containing protease inhibitors for 30 min. The lysates were then centrifuged and the supernatants collected. Approximately 40 μg of total protein was denatured and separated by 10% SDS-PAGE, and then transferred to a nitrocellulose membrane. The membranes were blocked with 5% non-fat milk in Tris-buffered saline containing 0.1% Tween-20 (TBST) for 2 hours at room temperature. The membranes were then incubated with the following primary antibodies overnight at 4°C: PCNA (Abcam, USA), pan Cytokeratin/AE1/AE3, Vimentin (Santa Cruz Biotechnology, USA), E-cadherin, p-MEK1/2(Ser217/221), MEK1/2, p-ERK1/2(Thr202/204), p-SAPK/JNK(Thr183/Tyr185), SAPK/JNK, p-p38 MAPK(Thr180/Tyr182), p38 MAPK, ERK1/2 (Cell Signaling Technology, USA), MMP2 and MMP9 (Boster Biological Technology, Wuhan, China). P-actin (Santa Cruz Biotechnology) was used as a loading control. The membranes were washed five times with TBST and then incubated with horseradish peroxidase-conjugated secondary antibodies for 1 hour at room

temperature. The signals were visualized using an Enhanced Chemiluminescence Detection Kit (Pierce Biotechnology, USA).

2.6. Quantitative real-time PCR

Total RNA was isolated from cells using the Qiagen RNeasy Mini Kit in combination with on-column DNase treatment (Applied Biosystems, USA). A High Capacity RNA-to-cDNA Kit (Applied Biosystems) was used to synthesize the first strand of cDNA. Quantitative real-time PCR was performed using the Power SYBR Green PCR Master Mix (Applied Biosystems) with gene-specific primers. The primers were the following: *E-cadherin*, 5'-TGG AGG AAT TCT TGC TTT GC-3' (F), 5'-CGC TCT CCT CCG AAG AAA C-3' (R); *Vimentin*, 5'-GGC TCG TCA CCT TCG TGA AT-3' (F), 5'-GAG AAA TCC TGC TCT CCT CGC-3' (R); *MMP2*, 5'-GAG AAC CAA AGT CTG AAG AG-3' (F), 5'-GGA GTG AGA ATG CTG ATT AG-3' (R); *MMP9*, 5'-TGC CCG GAC CAA GGA TAC AG-3' (F), 5'-TCA GGG CGA GGA CCA TAG AG-3' (R); *PAD1*, 5'-GAG TGA TGG ACA CTC ATG GC-3' (F), 5'-CAGATGGTCAGCTTGCAGTT-3' (R); *PAD2*, 5'-TCT CAG GCC TGG TCT CCA T-3' (F), 5'-AAG ATG GGA GTC AGG GGA AT-3' (R); *PAD3*, 5'-AGC AAT GAC CTC AAC GAC AG-3' (F), 5'-TGA GGT AGA GCA CCG CAT AG-3' (R); *PAD4*, 5'-TCA CCT ACC ACA TCA GGC AT-3' (F), 5'-CAT GTT CCA CCA CTT GAA GG-3' (R); *SNAIL*, **5**'- GCT GCA GGA CTC TAA TCC AGA-3' (F), 5'-ATC TCC GGA GGT GGG ATG-3' (R), and *GAPDH*, 5'-ACC CAT CAC CAT CTT CCA GGA G-3'(F), 5'-GAA GGG GCG GAG ATG ATG AC-3' (R). All target gene transcripts were normalized to *GAPDH*, and the relative fold change in expression calculated using the $2^{-\Delta\Delta CT}$ method.

2.7. Immunoprecipitation Assay

Flag-tagged PAD1 in pcDNA3.1 (+) or control vector were transfected into HEK 293 cells together with His-tagged MEK1 using FuGENE 6 (Roche). The whole cell lysates were immunoprecipitated with anti-Flag M2 affinity gel (Sigma A2220). Immunoprecipitates were washed and analysed by western blot using anti-His (Sigma), anti-MEK1, and anti-Flag (Sigma) antibodies as indicated. Reciprocally, Flag-tagged PAD1 in pcDNA3.1 (+) was transfected into HEK 293 cells with or without His-tagged MEK1, and cell lysates were immunoprecipitated with anti-His antibody, followed by detection with anti-His, and anti-Flag antibodies. Enzymatically inactive mutant of PAD1, mutation of Cys^{645} into Ser^{645} (CS), in pcDNA3.1 (+) was used as a control as indicated.

2.8. Immunofluorescence staining

Cells were grown on glass slides in 12-well plates. After washing with PBS, cells were fixed with 4% paraformaldehyde for 30 min, then permeabilized with 0.1% Triton X-100 for 10 min and blocked with 10% goat serum/1% BSA in PBS for 1 h at room temperature. Primary antibody against E-cadherin, AE1/AE3, or Vimentin was added to the cells overnight at 4°C, and Fluor 546-conjugated goat anti-rabbit secondary antibody (Invitrogen) was employed to detect fluorescence. The nuclei were stained with DAPI (Vector Laboratories, Cambridgeshire, UK). Representative images were collected with LSM 510 laser scanning confocal microscope (Carl Zeiss). When indicated, MDA-MB-231 cells were transfected with Flag-PAD1 and His-MEK1 plasmids using FuGENE 6 (Roche). Forty-eight

hours later, cells were collected for immunofluorescence staining. Where indicated, MDA-MB-231 cells were transfected with Flag-PAD1 (WT) or Flag-PAD1 (CS), followed by immunofluorescence analysis.

2.9. PAD enzymatic activity assay

MEK1 proteins were expressed and purified from pET28b-MEK1 using Ni-NTA Protein Purification System (Qiagen) according to manufacturer's instructions. PAD1 proteins were expressed and purified from pcDNA3.1-Flag-PAD1 or pcDNA3.1-Flag-PAD1 (C645S) mutant using anti-Flag M2 affinity gel system (Sigma). The PAD assay was performed essentially as described previously [19]. The expressed MEK1 was treated with PAD1 in PAD buffer containing 50 mM Tris-HCl, pH 7.6, 4 mM DTT, 4 mM $CaCl_2$ at 37 °C for 4 hr. Citrullination of MEK1 was detected using an Anti-Citrulline (Modified) Detection Kit (Millipore 17–347, Billerica, MA). The mutant PAD1 (CS) was used as a negative control.

2.10. Xenograft tumor model in nude mice

All animal experiments were conducted according to the standard institutional guidelines of Nanjing Medical University (Nanjing, China). PAD1-depleted MDA-MB-231 cells or the control cells (1×10^7) were injected subcutaneously into the left upper flank of the 6-week-old female BALB/c nude mice. Six mice were used for PAD1-depleted cell injection and five for control cell injection. Tumor diameters are measured with digital calipers, and the tumor volume in mm^3 was calculated by the following formula: Volume=0.5× $(Width)^2$ × Length. Mice were sacrificed 8 weeks after injection under anesthesia. For the experiment examining the effect of PAD1 inhibitor on tumor growth, MDA-MB-231 cells (2×10^6) were injected subcutaneously into 10 female nude mice. The tumors were allowed to grow for 3 weeks. Mice were randomly assigned into treatment or control groups (n=5/group) and administered intra-peritoneal injections of either D-Cl-amidine (20 mg/kg/day) or PBS as a vehicle control every other day. Treatment continued for 4 weeks and the tumor volume was measured weekly by digital caliper.

2.11. Statistical analysis

All experiments were independently repeated at least three times. Data are presented as mean ± SD. Statistical evaluation for data analysis was determined by Student's t-test with *indicating means significantly different ($P<0.05$) from control.

3. Results

3.1. PAD1 expression is positively associated with TNBC

To determine the clinical significance of PAD1 in breast tumors, we first examined PAD1 mRNA levels in human breast cancer using Oncomine cancer microarray database (https://www.oncomine.org/resource) [37]. According to the datasets of Finak *et al* (P-value=9.44E-16, fold change=2.202) [38] and Turashvili *et al* (P-value=0.028, fold change=1.711) [39], PAD1 transcript levels were significantly elevated in clinical human breast cancer tissues compared to the normal tissues. Additionally, we queried the breast cancer dataset in the Cancer Genome Atlas database (TCGA, https://tcga-data.nci.nih.gov/tcga/) and observed a 1.110 fold increase in PAD1 levels in breast cancer tissue compared to

normal breast tissue (P-value=0.035) (Fig. 1A). However, PAD1 transcript levels were not significantly upregulated in TNBC tissues in Gluck *et al* dataset compared to the normal controls, as a result of a limited number of normal breast samples in the dataset. It is noteworthy that PAD1 transcript level in Non-TNBC tissues varies greatly from cases in Gluck *et al* dataset, but the expression of PAD1 was still obviously higher in Non-TNBC tissues than that in the normal controls (Supplementary Fig. S1). We next asked whether there is a stronger association of PAD1 with TNBC than with other non-TNBC. Analysis of PAD1 expression in the Gluck *et al* dataset [40] clearly showed that PAD1 mRNA was significantly increased in TNBC samples compared with the non-TNBC cancer tissues (P-value=0.022) (Fig. 1B). To confirm these findings, we compared PAD1 protein levels in clinical TNBC and non-TNBC tumor tissues using immunohistochemistry. We found that PAD1 staining was positive in 4 out of 5 TNBC tumor sections (representative images shown in Fig. 1C) or normal human breast tissues (Supplementary Fig. S2), while none of the 5 non-TNBC tumor sections stained positive for PAD1. Our western blot result further confirmed that PAD1 expression with the right molecular weight is upregulated in the clinical TNBC tissues compared to the normal controls (Supplementary Fig. S3). These results suggest that PAD1 is upregulated in human breast cancer and is positively correlated with TNBC.

3.2. Knockdown or inhibition of PAD1 decreases TNBC cancer cell proliferation, migration and invasion

To strengthen the hypothesis that PAD1 is primarily expressed in TNBC cells and not in other breast cancer subtypes, we compared PAD1 expression levels in MDA-MB-231cells (ER-, PR-, HER2-) with MCF-7 (ER+, PR+, HER2-), MCF-10DCIS (ER-, PR-, HER2+), and the non-tumorigenic normal human breast epithelial cell line, MCF-10A. Consistent with our clinical findings, PAD1 mRNA was sharply elevated in the TNBC MDA-MB-231 line compared to the other breast cancer cell lines (Fig. 2A). Interestingly, PAD1 was the only PAD family member that was strongly expressed in MDA-MB-231 cells (Fig. 2B), further supporting the restricted expression pattern of PAD1 with respect to breast cancer subtype.

To study the role of PAD1 in TNBC carcinogenesis, we then generated PAD1-depleted MDA-MB-231 cell line using a lentiviral approach. PAD1 knockdown efficiency was confirmed via western blotting (Fig. 2C). Interestingly, we found that expression of the cell proliferation marker PCNA was also significantly reduced following PAD1 depletion, suggesting that PAD1 may play a direct role in the proliferation of MDA-MB-231 cells (Fig. 2C). We tested this hypothesis and found that PAD1 depletion suppressed MDA-MB-231 cell proliferation in 2D monolayer cultures (Fig. 2D) and also suppressed the anchorage-independent growth of MDA-MB-231 cells (Fig. 2E). We next examined the effect of PAD1 knockdown on MDA-MB-231 cell migration using wound-healing assays. Results show that PAD1 depletion significantly reduced the ability of MDA-MB-231 cells to migrate into the wound compared to the controls (Fig. 2F). We then performed transwell invasion assays across a Matrigel membrane and found that PAD1 depletion significantly decreased the ability of MDA-MB-231 to migrate across the gel matrix into the adjacent chamber (Fig. 2G). Quantitation of this result by measuring the optical density (OD) of the invaded cells is

shown in Fig. 2G (bottom row). To help answer whether PAD1 enzymatic activity contributes to these biological phenotypes, we treated MDA-MB-231 cells with a newly developed arginine-based PAD1 inhibitor, D-Cl-amidine, which has been shown to effectively inhibit PAD1 activity in breast cancer cell lines [41]. Results showed that inhibiting PAD1 activity significantly inhibited cell proliferation (Supplementary Fig. S4A). Changes in the wound healing areas were also suppressed in D-Cl-amidine-treated cells compared to the controls (Supplementary Fig. S4B). The effects of PAD1 inhibition on MDA-MB-231 cell migration and invasion were further analyzed using a Transwell system. As shown in Supplementary Fig. S4C, D-Cl-amidine significantly suppressed invasion of the cells through the membranes of the Transwell chambers. Taken together, these results suggest that PAD1 is required for the proliferation, migration and invasion of MDA-MB-231 cells.

3.3. Silencing PAD1 reverses the EMT in TNBC cells and correlates with a decrease in MMP2/9 expression

EMT is a critical early event involved in invasion and metastasis of cancers, characterized by loss of epithelial markers with a concomitant upregulation of mesenchymal markers [42]. To investigate whether PAD1 affects EMT, we evaluated the expression of E-cadherin and pan-cytokeratin (epithelial markers), Vimentin and Snail (mesenchymal markers). Knockdown of PAD1 resulted in a significant increase in expression of epithelial markers and a decrease in expression of mesenchymal markers at both the mRNA and protein levels (Fig. 3A–C). Inhibiting PAD1 enzymatic activity with D-Cl-amidine also resulted in a decrease in expression of Vimentin and an increase of E-cadherin (Supplementary Fig. S5). We also evaluated E-cadherin expression upon PAD1 knockdown or overexpression in another TNBC cell line, MDA-MB-468. As expected, PAD1 silencing increased E-cadherin expression (Fig. 3D) while exogenous expression of PAD1 led to a dramatic decrease in E-cadherin expression (Fig. 3E). Together, these results suggested that downregulation of PAD1 reverses the EMT progress in TNBC cells.

MMP2 and MMP9 play a critical role in the invasion and metastasis of malignant tumor cells, and overexpression of these factors has been positively correlated with an aggressive malignant phenotype and poor outcome of breast cancer patients [9,10]. Given that PAD1 is strongly associated with the EMT in TNBC tumor cells, we then asked whether PAD1 may play a role in regulation of MMP2/9 expression in TNBC cells. To this end, we first examined MMP2/9 gene expression upon PAD1 knockdown in MDA-MB-231 cells. Results showed a significant decrease of MMP2/9 expression at both the mRNA and protein levels compared to the control cells (Fig. 3F and G). Next, we tested the effect of inhibition of PAD1 enzymatic activity on MMP2/9 expression using D-Cl-amidine. As shown in Fig. 3H, D-Cl-amidine treatment strongly inhibited both MMP2 and MMP9 expression at the mRNA levels in MDA-MB-231 cells, with MMP2 being more completely inhibited. We also observed the same inhibitory effect of D-Cl-amidine on MMP2/9 expression at the protein levels by western blotting analysis (Fig. 3I). These observations suggested that PAD1 activity may be required for regulating the expression of MMP2/9 in MDA-MB-231 cells, therefore facilitating TNBC cell growth, migration and invasion.

3.4. PAD1 facilitates MMP2 and MMP9 expression through inactivation of MAPK signaling

Regulation of MMP2/9 expression involves multiple signaling cascades, particularly the mitogen-activated protein kinase (MAPK) signal transduction pathway [43,44]. Additionally, MAPK/MMP signaling pathway has been found to contribute to the invasive and metastatic potential of the highly invasive breast cancer cells, such as MDA-MB-231 [45]. Given these observations and that PAD1 is required for regulating the expression of both MMP2 and MMP9 in MDA-MB-231 cells, we wondered if PAD1 could also play a role in modulating MAPK signaling pathway which, in turn, may regulate MMP2/9 expression. Therefore, we first assessed the phosphorylation status of ERK1/2, P38, and JNK in PAD1 knockdown MDA-MB-231 cells. Results showed that silencing PAD1 led to a significant increase of ERK1/2 and P38 phosphorylations, while having no apparent effect on JNK phosphorylation (Fig.4A). Next, we treated cells with D-Cl-amidine and then tested whether inhibition of PAD1 enzymatic activity could also induce the activation of ERK1/2 and P38. We found that, while levels of unmodified ERK1/2 and P38 were not altered by D-Cl-amidine treatment, levels of phosphorylated ERK1/2 and P38 began to increase approximately 9 hours following treatment (Fig. 4B). These results suggested that PAD1 activity suppresses ERK1/2 and P38 MAPK activation in MDA-MB-231 cells.

To further explore the potential role of PAD1 in ERK1/2 and P38-regulated MMP2/9 downregulation, we treated both shRNA control and PAD1 knockdown MDA-MB-231 cells with either the MEK1/2 inhibitor U0126 (which specifically blocks ERK1/2 phosphorylation) or with the P38 MAPK inhibitor SB203580. Results showed that U0126 dramatically inhibited ERK1/2 phosphorylation in both cell lines (Fig. 4C) and that SB203580 could also inhibit P38 activation to a lesser extent (Fig. 4D). Due to the low levels of phosphorylated ERK1/2 and P38 in the control cells, further inhibition of ERK1/2 and P38 activity by either U0126 or SB203580 treatment did not seem to affect the expression of MM2/9 (Fig. 4E and 4F). However, the decreased expression of MMP2 repressed in PAD1 knockdown cells was significantly upregulated after U0126 treatment (Fig. 4E), suggesting that blocking ERK1/2 activation in PAD1 knockdown cells is responsible for upregulation of MMP2 expression, while blocking P38 activation with SB203580 had no obvious effect on MMP2 expression (Fig. 4F). Given our previous results showing that either depletion or inhibition of PAD1 led to a significant increase of ERK1/2 (Fig. 4A and B), it is possible that depletion of PAD1 promotes ERK1/2 phosphorylation, whereas U0126 treatment inhibits this activation, thus partly reversing the MMP2 level. When we examined MMP9 expression under the same condition, we found that MMP9 did not seem to be affected after U0126 treatment (Fig. 4E). However, inhibition of P38 activation in the PAD1 knockdown cells slightly elevated MMP9 expression level, though it was not statistically significant (Fig. 4F). Together, our results suggested that PAD1 may facilitate MMP2 expression specifically through inhibiting ERK1/2 signaling, and partially regulate MMP9 expression via inhibiting P38 MAPK pathway in MDA-MB-231 cells.

3.5. PAD1 interacts with MEK1 and then targets MEK1 for citrullination

The MAPK pathway represents a cascade of phosphorylation events including three pivotal kinases, namely Raf, MEK (MAP kinase kinase), and ERK (MAP kinase) [43,44]. Given the striking correlation between PAD1 and ERK1/2 activation in mediating MMP2 expression,

we wondered whether PAD1 may target MEK to regulate ERK1/2 phosphorylation. To test this hypothesis, we first confirmed the phosphorylated MEK was not activated in PAD1 knockdown cells, which suggested that PAD1 does not affect Raf-mediated MEK activation (Fig. 5A). We next carried out co-immunoprecipitation analysis to test whether PAD1 and MEK1/2 interact. We transiently transfected Flag-tagged PAD1 and His-tagged MEK1 into HEK293 cells and immunoprecipitated with anti-Flag antibody. As shown in Fig. 5B, a substantial amount of MEK1 was co-precipitated from cells expressing both PAD1 and MEK1. Reciprocally, we also found that the overexpressed His-tagged MEK1 was immunoprecipitated with the anti-His antibody, and the coprecipitated PAD1 proteins were subsequently detected using the anti-Flag antibody (Fig. 5C). Furthermore, we performed immunofluorescence analysis in MDA-MB-231 cells transfected with Flag-tagged PAD1 and His-tagged MEK1 plasmids and found a strong co-localization between exogenously expressed PAD1 and MEK1 (Fig. 5D). These results demonstrated that PAD1 can physically associate with MEK1.

The findings that PAD1 interacted with MEK1 and that inhibition of PAD1 elevated phosphorylation of ERK1/2 (but not MEK1) suggested that PAD1 may target MEK1 to negatively regulate MEK1 enzyme activity, thus suppressing the subsequent phosphorylation of ERK1/2 by MEK1. Several studies from others and us have shown that, in addition to targeting histones [18–20], PAD4 can also regulate to function on non-histone proteins via citrullination [22–26,29]. We therefore wondered whether PAD1 could modulate MEK1 via similar mechanisms. To test this hypothesis, His-tagged MEK1 was purified, treated with recombinant PAD1 (WT or C645S enzymatic mutation), and the resolved proteins were then probed with an antibody that is reactive with citrullinated proteins (anti-Pan-Cit) as previously described [46]. This antibody was specifically designed to detect deiminated proteins (citrulline residues) regardless of the backbone protein molecules on polyvinylidene difluoride membranes [46]. Results (Fig. 5E) showed that the anti-Pan-Cit antibody was reactive with an appropriately sized band (45 kDa) from the anti-MEK1 immunoprecipitate (lane 3) and was not reactive with proteins that had been treated with the PAD1 CS mutant (lane 2) or from proteins without PAD1 treatment (lanes 1). These results support the hypothesis that MEK1 is a target for PAD1-mediated citrullination.

3.6. Inactivating PAD1 enzymatic activity facilitates MEK-ERK1/2 signaling activation

PAD-mediated citrullination can alter the tertiary structure of target substrates and/or mediate wide-ranging effects on protein-protein interactions and protein function, thus affecting various cellular processes [17,22–26,29]. Given that PAD1 appears to target MEK1 for citrullination, we wondered whether citrullination of MEK1 could also affect the protein interaction between PAD1 and MEK1. To test this hypothesis, we transiently transfected both Flag-tagged PAD1 and His-tagged MEK1 in HEK293 cells and then performed co-immunoprecipitation analysis with anti-Flag antibody. As shown in Fig. 5F, a substantial amount of MEK1 was co-precipitated from cells expressing wild-type PAD1, while this interaction dramatically decreased in cells transfected with the C645S mutant. These results confirmed that MEK1 citrullination is required for the physical interaction between PAD1 and MEK1, while catalytically inactive PAD1 failed to citrullinate MEK1 and therefore lost the ability to form a stable interaction between these two proteins.

To further investigate whether MEK1 citrullination directly inactivates MEK1-catalyzed ERK1/2 phosphorylation, we first performed immunofluorescence analysis in MDA-MB-231 cells transfected with either WT or CS PAD1 and then compared the status of ERK1/2 activation in these cells. Exogenous expression of Flag-tagged PAD1 did not cause an increase in the ERK1/2 phosphorylation above the basal level, whereas a significant increase of phosphorylated ERK1/2 was observed only in the cells transfected with CS PAD1 (Fig. 5G). We also examined the status of ERK1/2 activation by western blotting, and the results confirmed an increased p-ERK1/2 level upon CS PAD1 overexpression (Supplementary Fig. S6A). Next, we performed MEK1 *in vitro* kinase assays on ERK1/2 with either WT or CS PAD1. As shown in Supplementary Fig. S6B, higher levels of p-ERK1/2 was only observed following pretreatment of MEK1 with CS PAD1 when compared to pretreatment with WT PAD1. Collectively, these results support the hypothesis that phosphorylation of ERK1/2 by MEK1 is dependent on the enzymatic activity of PAD1.

3.7. PAD1 is essential for tumor growth and tumor metastasis of TNBC in mice

To confirm the *in vitro* phenotype of TNBC cells upon PAD1 knockdown, we first examined the effect of silencing PAD1 on tumor growth in xenograft mouse model of TNBC. The mice inoculated with PAD1 knockdown cells all exhibited smaller tumors than the control mice and this difference became significant 7 weeks post cell injection (Fig.6A). Next, we tested whether treatment of mice with PAD1 inhibitor would suppress the growth of MDA-MB-231-derived tumors. Results showed that D-Cl-amidine treatment caused a significant reduction in the size of the tumors (Fig. 6B). We also confirmed the knockdown efficiency of PAD1 in established tumors by western blotting. As expected, the tumors in mice inoculated with PAD1 KD cell lines had diminished expression of PAD1 (Fig. 6C). Moreover, the expression level of Ki67, a proliferation marker, was dramatically decreased in these PAD1 KD tumors, further supporting the tumor growth defect from the PAD1 KD cells (Fig. 6D). To test whether the difference of tumor growth is dependent on MEK1 activity and MMP2/9 expression, we compared the ERK1/2 activation and MMP2/9 expressions in the xenograft mouse tumor samples. Results showed that p-ERK1/2 was activated and expression levels of MMP2/9 were downregulated in tumors from the mice inoculated with PAD1 KD cells compared to the controls (Supplementary Fig. S7). These results suggest that the PAD1-ERK1/2-MMP2 pathway is involved in the regulation of TNBC tumor growth. Importantly, two mice injected with the control MDA-MB-231 cell developed tumor metastases in livers, with small hepatic nodules (arrow) spreading throughout the liver surface, whereas no such metastasis was observed in mice injected with PAD1 KD cells (Fig. 6E). Histological analysis on the livers confirmed the metastasis foci in the shRNA control tumors (Fig. 6F). Collectively, these data suggested that PAD1 promoted the tumorigenesis and metastatic process of TNBC cells *in vivo*.

4. Discussion

Accumulating evidence is now linking the PAD enzyme family with carcinogenesis and tumor progression [17,30–34]. However, apart from a previous study which identified PAD1 as a potential biomarker for the early detection of invasive oral squamous cell carcinoma [47], no previous studies have experimentally investigated the tumorigenic potential of

PAD1. To broaden our knowledge of the role of PAD1 in breast cancer, we evaluated PAD1 expression in both the Oncomine breast cancer database and in the TCGA tumor database and results show that the expression of PAD1 is upregulated in breast cancer patients and positively correlated with TNBC. These findings suggest that PAD1 may be involved in regulating TNBC progression. To test this hypothesis, we utilized MDA-MB-231 cells as a well-established TNBC cell model, and found that PAD1 was highly expressed in this cell line relative to cell models of other types of breast cancer. We next investigated the role of PAD1 knockdown on TNBC cell malignant behavior and found that depletion of PAD1 suppressed the ability of MDA-MD-231 cells to proliferate, migrate, and invade *in vitro*, and also suppressed the ability of MDA-MB-231 tumors to grow and metastasize *in vivo*. In addition, PAD1 knockdown or inhibition also reversed EMT process in MDA-MB-231 cells. These findings suggest that PAD1 may promote tumor metastasis in TNBC by promoting the EMT.

EMT is critically important for the first steps of the metastatic process [42] and MMP2/9 have been found to facilitate this activity [9,10]. The potential role for PAD1 in regulating MMP2/9 expression is partially clarified when the above findings are put in the context of what is currently known about the role of MAPK signaling in this process. MAPKs, which belong to a large family of evolutionarily conserved serine/threonine kinases, represent one of the signaling cascades that link extracellular signals to the transcriptional regulation of various molecules that control cell proliferation, growth, migration, and invasion in various cell types, including cancer cells [6,48]. In mammals, at least three major MAPK protein kinases have been identified: ERK, P38, and JNK/SAPK [48]. These signaling pathways have been studied extensively for their roles in regulating MMP2/9 expression in human breast cancers, especially ERK [43–45]. In our study, we show that both ERK1/2 and P38 are activated in PAD1 depleted or inhibitor-treated lines, suggesting an inhibitory effect of PAD1 on ERK1/2 and P38 activation. Given our observation that MMP2/9 expression is concomitantly downregulated upon PAD1 depletion or inhibition, it is possible that PAD1 depletion or inhibition facilitates the activation of ERK1/2 and P38 MAPKs, which negatively regulate MMP2/9 expression. We also provide evidence showing that ERK1/2 and P38 play distinct roles in MMP2/9 regulation in PAD1 depleted MDA-MB-231 cells. ERK1/2 inactivation appears to primarily be responsible for upregulation of MMP2 expression in PAD1 knockdown cells, while having no effect on MMP9 expression. Our data are in line with recent studies showing that inhibiting ERK1/2 activity leads to a significant increase in the expression of MMP2 transcript in cardiac myocytes, while the inhibition of P38 increases MMP-9 in fibrosarcoma cells [5,6]. However, despite numerous independent studies, the precise role of MAPK signaling in regulating MMP2/9 expression remains controversial [43–45]. Though inhibition of P38 MAPK may partially be involved in the decrease of MMP9, the possibility that additional signaling pathways contribute to the MMP9 regulation in PAD1 knockdown cells cannot be excluded, particularly since inhibiting P38 phosphorylation does not significantly reverse the decreased expression of MMP9 upon PAD1 depletion. Previous studies have provided strong evidence showing that phosphatidylinositol 3-kinase/Akt and nuclear factor-κB pathways play critical roles in the modulation of MMP9 expression [49,50]. In future studies, we will investigate these signaling pathways in our PAD1-depleted MDA-MB-231 cells.

While our data show that PAD1 is involved in regulating MMP2/9 expression through MAPK signaling, we also wanted to know how PAD1 modulates MAPK activity. Given that PAD1 depletion does not affect Raf-mediated MEK1 phosphorylation (but elevates MEK1-mediated ERK1/2 activation), that PAD1 interacts with MEK1, and that citrullination catalyzed by PAD4 can alter protein-protein interactions [22–26,29], we proposed that PAD1 may be involved in inhibiting ERK1/2 phosphorylation by directly targeting MEK1 for citrullination, which negatively regulates MEK1 enzyme activity. To make this conclusion, we first demonstrated that PAD1 can citrullinate MEK1 *in vitro*. Next, our finding that enzymatically inactive PAD1 dramatically dampens the PAD1-MEK1 interaction suggested that MEK1 citrullination is required for the physical interaction between PAD1 and MEK1. Further, we demonstrated that MEK1 citrullination by PAD1 directly inactivates MEK1-mediated ERK phosphorylation. Our finding that citrullination of MEK1 has an impact on inter-protein binding capability fits well with the previous report showing that citrullination of p300 by PAD4 can restore or enhance the biomolecular interaction of p300 to its binding protein, and therefore may cause conformational changes in the p300 complex which facilitates subsequent steps in the transcriptional activation process [24]. It is also worth noting that citrullination of ING4 (a tumor suppressor protein) by PAD4 disrupts the interaction between ING4 and p53, thus suppressing the ability of ING4 to promote p53 acetylation [29]. We believe that the role of PAD-mediated citrullination is much more complicated than originally thought and this enzymatic activity probably occurs in a cell-type and context-specific nature [22,23,25,26]. Therefore, it is conceivable that, in MDA-MB-231 cells, PAD1 binds and catalyzes MEK1 for citrullination, which, in turn, strengthens the interaction between PAD1 and MEK1, thus preventing the phosphorylation activity of MEK1 on its downstream target ERK1/2. Upon PAD1 knockdown, citrullination of MEK1 is then deficient, leading to less stable interaction between PAD1 and MEK1, and subsequent ERK1/2 activation.

The inhibition of MMP2/9 expression and secretion is important to prevent cell adhesion, migration, invasion and metastasis [9,10]. Our results showing that PAD1 depletion or inhibition reduced MMP2 and MMP9 expression is of particular interest because the loss or down-regulation of MMP2/9 could potentially reverse the EMT phenotype, thereby leading to a less aggressive tumor phenotype and better outcomes for breast cancer patients [10]. Our result is in line with several previous reports which also investigated inhibition of MMP2/9 by other chemicals such as oleamide [51], Emodin [52], or FePP [53], for 24-hour treatment in MDA-MB-231 cells, all leading to the decreased cell migration, invasion and metastasis. In this regard, it seems reasonable to suggest that PAD1 may function as an early stage prognostic biomarker and therapeutic target for TNBC. Currently, there are no specific treatment guidelines for TNBC and most clinical antitumor agents are prone to tumor resistance and cell toxicity. Therefore, novel anti-TNBC agents targeting tumor cell migration and invasion are urgently needed [54]. Our finding that PAD1 specific inhibitor, D-Cl-amidine, is successful in suppressing tumor growth in a xenograft mouse model of TNBC together with our previous *in vitro* study showing that D-Cl-amidine also effectively inhibits cell viability [41], suggests that inhibiting PAD1 could potentially be utilized as a good strategy to treat metastatic breast cancer. Further studies aimed at developing PAD1-selective inhibitors and then evaluating the pharmacokinetics, biodistribution, and anti-tumor

effects of these compounds in preclinical models of cancer will represent important next steps towards advancing our overall goals.

Supplementary Material

Refer to Web version on PubMed Central for supplementary material.

Acknowledgments

This work was supported by the National Natural Science Foundation of China (81372850), the Key University Natural Science Research Project of Jiangsu Province (15KJA320003), Jiangsu SixTalent Peaks, and Jiangsu Entrepreneurship & Innovation Award. Work in the Thompson lab is supported by NIGMS grant GM118112.

References

1. Foulkes WD, Smith IE, Reis-Filho JS. Triple-negative breast cancer. The New England journal of medicine. 2010; 363:1938–48. [PubMed: 21067385]
2. Elias AD. Triple-negative breast cancer: a short review. American journal of clinical oncology. 2010; 33:637–45. [PubMed: 20023571]
3. Yilmaz M, Christofori G, Lehembre F. Distinct mechanisms of tumor invasion and metastasis. Trends in molecular medicine. 2007; 13:535–41. [PubMed: 17981506]
4. Chabottaux V, Noel A. Breast cancer progression: insights into multifaceted matrix metalloproteinases. Clinical & experimental metastasis. 2007; 24:647–56. [PubMed: 17968664]
5. Spallarossa P, Altieri P, Garibaldi S, Ghigliotti G, Barisione C, Manca V, et al. Matrix metalloproteinase-2 and −9 are induced differently by doxorubicin in H9c2 cells: The role of MAP kinases and NAD(P)H oxidase. Cardiovascular research. 2006; 69:736–45. [PubMed: 16213474]
6. Gweon EJ, Kim SJ. Resveratrol induces MMP-9 and cell migration via the p38 kinase and PI-3K pathways in HT1080 human fibrosarcoma cells. Oncology reports. 2013; 29:826–34. [PubMed: 23229870]
7. Sato H, Takino T, Okada Y, Cao J, Shinagawa A, Yamamoto E, et al. A matrix metalloproteinase expressed on the surface of invasive tumour cells. Nature. 1994; 370:61–5. [PubMed: 8015608]
8. Hidalgo M, Eckhardt SG. Development of matrix metalloproteinase inhibitors in cancer therapy. Journal of the National Cancer Institute. 2001; 93:178–93. [PubMed: 11158186]
9. Radisky ES, Radisky DC. Matrix metalloproteinase-induced epithelial-mesenchymal transition in breast cancer. Journal of mammary gland biology and neoplasia. 2010; 15:201–12. [PubMed: 20440544]
10. Kohrmann A, Kammerer U, Kapp M, Dietl J, Anacker J. Expression of matrix metalloproteinases (MMPs) in primary human breast cancer and breast cancer cell lines: New findings and review of the literature. BMC cancer. 2009; 9:188. [PubMed: 19531263]
11. Minn AJ, Gupta GP, Siegel PM, Bos PD, Shu W, Giri DD, et al. Genes that mediate breast cancer metastasis to lung. Nature. 2005; 436:518–24. [PubMed: 16049480]
12. Gupta GP, Nguyen DX, Chiang AC, Bos PD, Kim JY, Nadal C, et al. Mediators of vascular remodelling co-opted for sequential steps in lung metastasis. Nature. 2007; 446:765–70. [PubMed: 17429393]
13. van ‘t Veer LJ, Dai H, van de Vijver MJ, He YD, Hart AAM, Mao M, et al. Gene expression profiling predicts clinical outcome of breast cancer. Nature. 2002; 415:530–6. [PubMed: 11823860]
14. Vossenaar ER, Zendman AJ, van Venrooij WJ, Pruijn GJ. PAD, a growing family of citrullinating enzymes: genes, features and involvement in disease. BioEssays : news and reviews in molecular, cellular and developmental biology. 2003; 25:1106–18.
15. Chavanas S, Mechin MC, Takahara H, Kawada A, Nachat R, Serre G, et al. Comparative analysis of the mouse and human peptidylarginine deiminase gene clusters reveals highly conserved non-coding segments and a new human gene, PADI6. Gene. 2004; 330:19–27. [PubMed: 15087120]

16. Ellsworth RE, Vertrees A, Love B, Hooke JA, Ellsworth DL, Shriver CD. Chromosomal alterations associated with the transition from in situ to invasive breast cancer. Annals of surgical oncology. 2008; 15:2519–25. [PubMed: 18622645]
17. Chang X, Han J. Expression of peptidylarginine deiminase type 4 (PAD4) in various tumors. Molecular carcinogenesis. 2006; 45:183–96. [PubMed: 16355400]
18. Guertin MJ, Zhang X, Anguish L, Kim S, Varticovski L, Lis JT, et al. Targeted H3R26 deimination specifically facilitates estrogen receptor binding by modifying nucleosome structure. PLoS genetics. 2014; 10:e1004613. [PubMed: 25211228]
19. Wang Y, Wysocka J, Sayegh J, Lee YH, Perlin JR, Leonelli L, et al. Human PAD4 regulates histone arginine methylation levels via demethylimination. Science (New York, NY). 2004; 306:279–83.
20. Yao H, Li P, Venters BJ, Zheng S, Thompson PR, Pugh BF, et al. Histone Arg modifications and p53 regulate the expression of OKL38, a mediator of apoptosis. The Journal of biological chemistry. 2008; 283:20060–8. [PubMed: 18499678]
21. Li P, Yao H, Zhang Z, Li M, Luo Y, Thompson PR, et al. Regulation of p53 target gene expression by peptidylarginine deiminase 4. Molecular and cellular biology. 2008; 28:4745–58. [PubMed: 18505818]
22. Stadler SC, Vincent CT, Fedorov VD, Patsialou A, Cherrington BD, Wakshlag JJ, et al. Dysregulation of PAD4-mediated citrullination of nuclear GSK3beta activates TGF-beta signaling and induces epithelial-to-mesenchymal transition in breast cancer cells. Proceedings of the National Academy of Sciences of the United States of America. 2013; 110:11851–6. [PubMed: 23818587]
23. Zhang X, Gamble MJ, Stadler S, Cherrington BD, Causey CP, Thompson PR, et al. Genome-wide analysis reveals PADI4 cooperates with Elk-1 to activate c-Fos expression in breast cancer cells. PLoS genetics. 2011; 7:e1002112. [PubMed: 21655091]
24. Lee YH, Coonrod SA, Kraus WL, Jelinek MA, Stallcup MR. Regulation of coactivator complex assembly and function by protein arginine methylation and demethylimination. Proceedings of the National Academy of Sciences of the United States of America. 2005; 102:3611–6. [PubMed: 15731352]
25. Tanikawa C, Ueda K, Nakagawa H, Yoshida N, Nakamura Y, Matsuda K. Regulation of protein Citrullination through p53/PADI4 network in DNA damage response. Cancer research. 2009; 69:8761–9. [PubMed: 19843866]
26. Deplus R, Denis H, Putmans P, Calonne E, Fourrez M, Yamamoto K, et al. Citrullination of DNMT3A by PADI4 regulates its stability and controls DNA methylation. Nucleic acids research. 2014; 42:8285–96. [PubMed: 24957603]
27. Chang X, Yamada R, Sawada T, Suzuki A, Kochi Y, Yamamoto K. The inhibition of antithrombin by peptidylarginine deiminase 4 may contribute to pathogenesis of rheumatoid arthritis. Rheumatology (Oxford, England). 2005; 44:293–8.
28. Ordonez A, Yelamos J, Pedersen S, Minano A, Conesa-Zamora P, Kristensen SR, et al. Increased levels of citrullinated antithrombin in plasma of patients with rheumatoid arthritis and colorectal adenocarcinoma determined by a newly developed ELISA using a specific monoclonal antibody. Thrombosis and haemostasis. 2010; 104:1143–9. [PubMed: 20838745]
29. Guo Q, Fast W. Citrullination of inhibitor of growth 4 (ING4) by peptidylarginine deminase 4 (PAD4) disrupts the interaction between ING4 and p53. The Journal of biological chemistry. 2011; 286:17069–78. [PubMed: 21454715]
30. Chang X, Han J, Pang L, Zhao Y, Yang Y, Shen Z. Increased PADI4 expression in blood and tissues of patients with malignant tumors. BMC cancer. 2009; 9:40. [PubMed: 19183436]
31. Zheng Y, Zhao G, Xu B, Liu C, Li C, Zhang X, et al. PADI4 has genetic susceptibility to gastric carcinoma and upregulates CXCR2, KRT14 and TNF-alpha expression levels. Oncotarget. 2016; 7:62159–76. [PubMed: 27556695]
32. Cui YY, Yan L, Zhou J, Zhao S, Zheng YB, Sun BH, et al. The role of peptidylarginine deiminase 4 in ovarian cancer cell tumorigenesis and invasion. Tumour biology : the journal of the International Society for Oncodevelopmental Biology and Medicine. 2016; 37:5375–83. [PubMed: 26563365]

33. Wang H, Xu B, Zhang X, Zheng Y, Zhao Y, Chang X. PADI2 gene confers susceptibility to breast cancer and plays tumorigenic role via ACSL4, BINC3 and CA9 signaling. Cancer cell international. 2016; 16:61. [PubMed: 27478411]

34. McElwee JL, Mohanan S, Griffith OL, Breuer HC, Anguish LJ, Cherrington BD, et al. Identification of PADI2 as a potential breast cancer biomarker and therapeutic target. BMC cancer. 2012; 12:500. [PubMed: 23110523]

35. Wang Y, Li P, Wang S, Hu J, Chen XA, Wu J, et al. Anticancer peptidylarginine deiminase (PAD) inhibitors regulate the autophagy flux and the mammalian target of rapamycin complex 1 activity. The Journal of biological chemistry. 2012; 287:25941–53. [PubMed: 22605338]

36. Senshu T, Kan S, Ogawa H, Manabe M, Asaga H. Preferential deimination of keratin K1 and filaggrin during the terminal differentiation of human epidermis. Biochemical and biophysical research communications. 1996; 225:712–9. [PubMed: 8780679]

37. Rhodes DR, Kalyana-Sundaram S, Mahavisno V, Varambally R, Yu J, Briggs BB, et al. Oncomine 3.0: genes, pathways, and networks in a collection of 18,000 cancer gene expression profiles. Neoplasia (New York, NY). 2007; 9:166–80.

38. Finak G, Bertos N, Pepin F, Sadekova S, Souleimanova M, Zhao H, et al. Stromal gene expression predicts clinical outcome in breast cancer. Nature medicine. 2008; 14:518–27.

39. Turashvili G, Bouchal J, Baumforth K, Wei W, Dziechciarkova M, Ehrmann J, et al. Novel markers for differentiation of lobular and ductal invasive breast carcinomas by laser microdissection and microarray analysis. BMC cancer. 2007; 7:55. [PubMed: 17389037]

40. Gluck S, Ross JS, Royce M, McKenna EF Jr, Perou CM, Avisar E, et al. TP53 genomics predict higher clinical and pathologic tumor response in operable early-stage breast cancer treated with docetaxel-capecitabine +/− trastuzumab. Breast cancer research and treatment. 2012; 132:781–91. [PubMed: 21373875]

41. Bicker KL, Anguish L, Chumanevich AA, Cameron MD, Cui X, Witalison E, et al. D-amino acid based protein arginine deiminase inhibitors: Synthesis, pharmacokinetics, and in cellulo efficacy. ACS medicinal chemistry letters. 2012; 3:1081–5. [PubMed: 23420624]

42. Lamouille S, Xu J, Derynck R. Molecular mechanisms of epithelial-mesenchymal transition. Nature reviews Molecular cell biology. 2014; 15:178–96. [PubMed: 24556840]

43. Cho HJ, Kang JH, Kwak JY, Lee TS, Lee IS, Park NG, et al. Ascofuranone suppresses PMA-mediated matrix metalloproteinase-9 gene activation through the Ras/Raf/MEK/ERK- and Ap1-dependent mechanisms. Carcinogenesis. 2007; 28:1104–10. [PubMed: 17114644]

44. Hong IK, Kim YM, Jeoung DI, Kim KC, Lee H. Tetraspanin CD9 induces MMP-2 expression by activating p38 MAPK, JNK and c-Jun pathways in human melanoma cells. Experimental & molecular medicine. 2005; 37:230–9. [PubMed: 16000878]

45. Wang L, Ling Y, Chen Y, Li CL, Feng F, You QD, et al. Flavonoid baicalein suppresses adhesion, migration and invasion of MDA-MB-231 human breast cancer cells. Cancer letters. 2010; 297:42–8. [PubMed: 20580866]

46. Senshu T, Sato T, Inoue T, Akiyama K, Asaga H. Detection of citrulline residues in deiminated proteins on polyvinylidene difluoride membrane. Analytical biochemistry. 1992; 203:94–100. [PubMed: 1524220]

47. Chen C, Mendez E, Houck J, Fan W, Lohavanichbutr P, Doody D, et al. Gene expression profiling identifies genes predictive of oral squamous cell carcinoma. Cancer epidemiology, biomarkers & prevention : a publication of the American Association for Cancer Research, cosponsored by the American Society of Preventive Oncology. 2008; 17:2152–62.

48. Dhillon AS, Hagan S, Rath O, Kolch W. MAP kinase signalling pathways in cancer. Oncogene. 2007; 26:3279–90. [PubMed: 17496922]

49. Wang YH, Dong YY, Wang WM, Xie XY, Wang ZM, Chen RX, et al. Vascular endothelial cells facilitated HCC invasion and metastasis through the Akt and NF-kappaB pathways induced by paracrine cytokines. Journal of experimental & clinical cancer research : CR. 2013; 32:51. [PubMed: 23941552]

50. Chien CS, Shen KH, Huang JS, Ko SC, Shih YW. Antimetastatic potential of fisetin involves inactivation of the PI3K/Akt and JNK signaling pathways with downregulation of MMP-2/9

expressions in prostate cancer PC-3 cells. Molecular and cellular biochemistry. 2010; 333:169–80. [PubMed: 19633975]

51. Zibara K, Awada Z, Dib L, El-Saghir J, Al-Ghadban S, Ibrik A, et al. Anti-angiogenesis therapy and gap junction inhibition reduce MDA-MB-231 breast cancer cell invasion and metastasis in vitro and in vivo. Scientific reports. 2015; 5:12598. [PubMed: 26218768]
52. Sun Y, Wang X, Zhou Q, Lu Y, Zhang H, Chen Q, et al. Inhibitory effect of emodin on migration, invasion and metastasis of human breast cancer MDA-MB-231 cells in vitro and in vivo. Oncology reports. 2015; 33:338–46. [PubMed: 25370743]
53. Lin CW, Shen SC, Hou WC, Yang LY, Chen YC. Heme oxygenase-1 inhibits breast cancer invasion via suppressing the expression of matrix metalloproteinase-9. Molecular cancer therapeutics. 2008; 7:1195–206. [PubMed: 18483307]
54. Eckhardt BL, Francis PA, Parker BS, Anderson RL. Strategies for the discovery and development of therapies for metastatic breast cancer. Nature reviews Drug discovery. 2012; 11:479–97. [PubMed: 22653217]

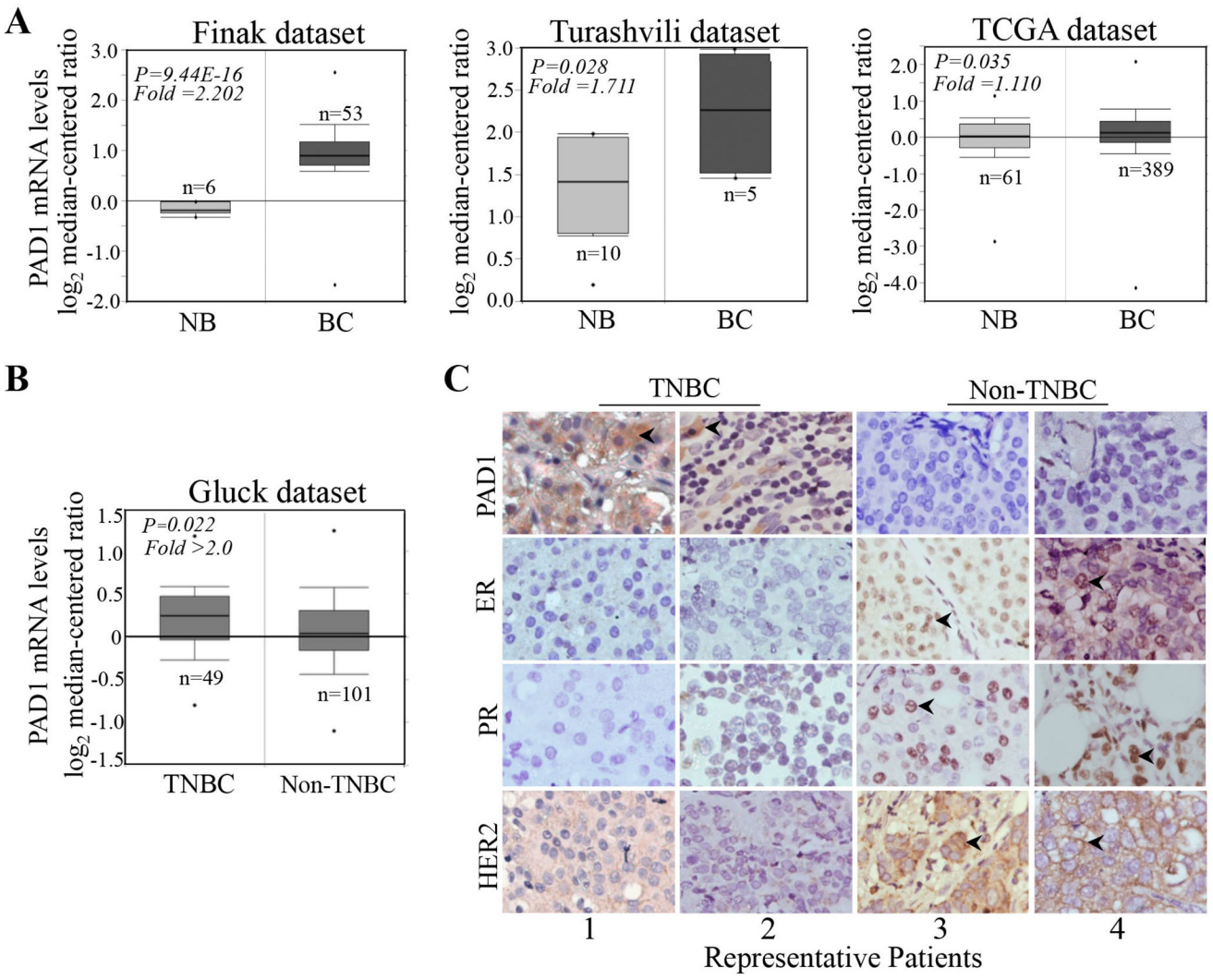

Figure 1. PAD1 mRNA expression in breast cancer microarray database

(A) Analysis of PAD1 mRNA levels in human breast carcinoma tissues compared with normal breast tissues in the Oncomine cancer microarray database and in the TCGA datasbase. Images were displayed as a boxplot (log_2 median-centered). The sample numbers are shown. P values were calculated using the Student *t* test. NB: normal breast tissue; BC: breast carcinoma. (B) PAD1 mRNA expression in triple negative breast cancer (TNBC) and non-TNBC tissues was analyzed in Gluck Oncomine database. (C) Expression levels of PAD1 were examined by immunohistochemistry staining. Representative sections from patients (TNBC, #1 and #2) who stained positive for PAD1 and negative for ER, PR, and HER2, and patients (non-TNBC, #3and #4) who stained negative for PAD1 and positive for ER, PR, and HER2. Black arrow head indicating the positive signals. Original magnification, ×100

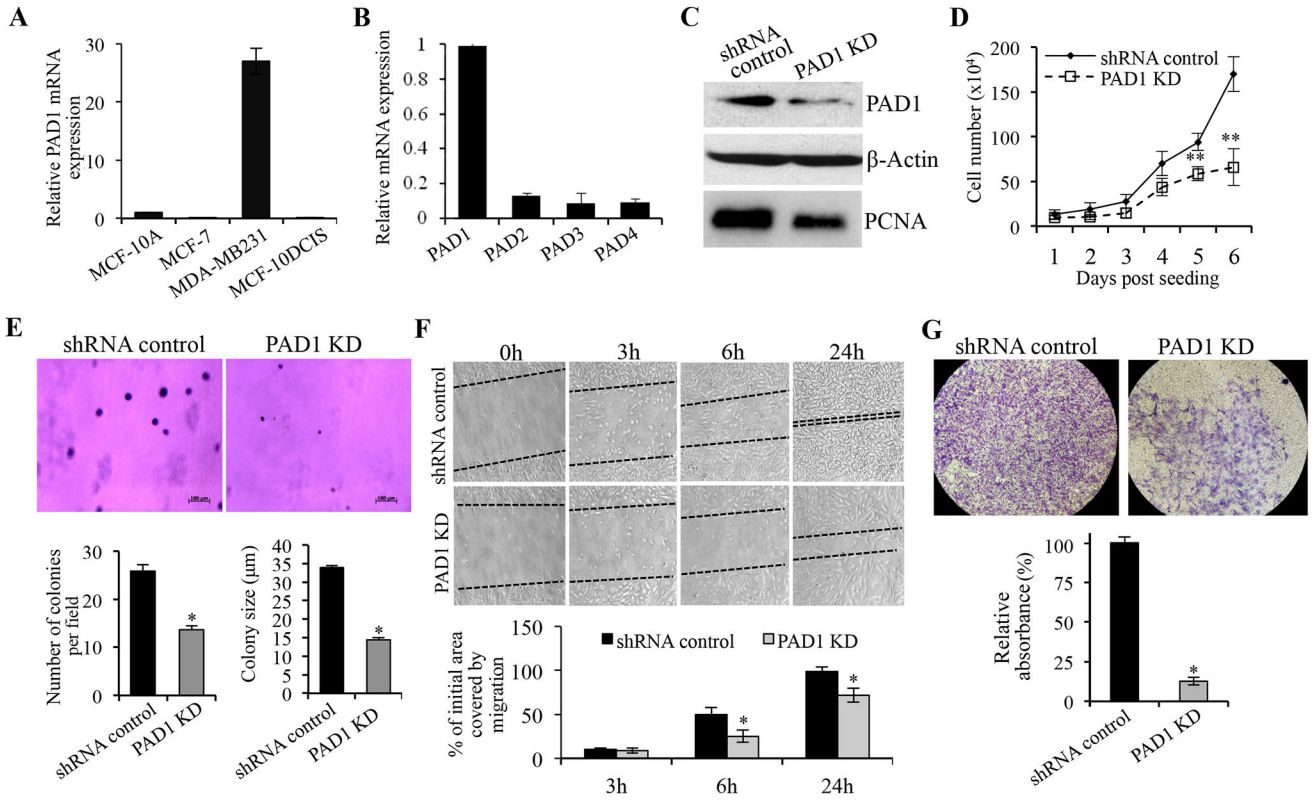

Figure 2. PAD1 enhances TNBC cell proliferation, migration and invasion

(A) Endogenous PAD1 mRNA levels in indicated breast cancer cell lines were determined by qRT-PCR. The mRNA levels of PAD1 in other cell lines were normalized to that in MCF-10A cells. GAPDH served as loading control. (B) Endogenous PAD1–4 mRNA levels in MDA-MB-231 cells were determined by qRT-PCR. The mRNA levels of PAD2–4 were normalized to that in MDA-MB-231 cells. (C) The representative immunoblot shows efficient PAD1 knockdown in MDA-MB-231 cells and the decreased PCNA expression upon depletion of PAD1. β-Actin served as loading control. (D) PAD1 knockdown or shRNA control MDA-MB-231 cells were cultured in regular medium, at indicated times, cell numbers were counted under light microscope. **P < 0.01. (E) PAD1 knockdown or shRNA control MDA-MB-231 cells were plated in soft agar and assayed for colony number after 3 weeks. The representative image was shown in the upper panel. Scale bar: 100 μm. The data were presented as the mean ± SD from three independent experiments (lower panel). *P < 0.05. (F) Wound healing assay was performed to detect the migratory capacity of MDA-MB-231 cells after PAD1 depletion. Representative images of wound closure assays at indicated hours after scratching were presented (upper panel). The data were presented as the mean ± SD from three independent experiments (lower panel). *P < 0.05. (G) Transwell assay was performed to evaluate the invasive potential of PAD1 KD cells or the shRNA control MDA-MB-231 cells. The representative image shows invasive cells that were fixed and stained with crystal violet (upper panel). The optical density of the invaded cells from shRNA control MDA-MB-231 cells was used as the normal 100%. The data were presented as the mean ± SD from three independent experiments (lower panel). *P < 0.05.

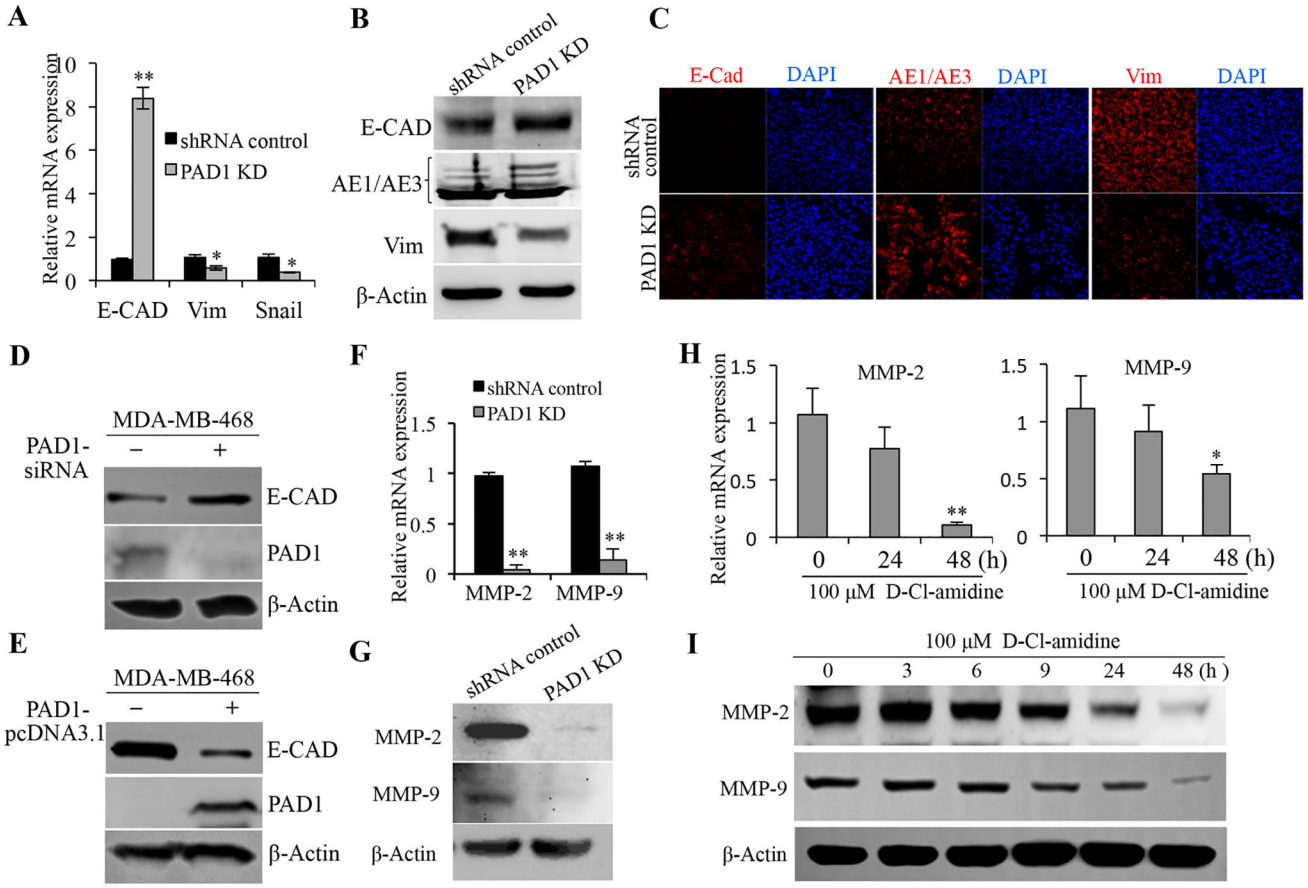

Figure 3. Silencing PAD1 reverses the epithelial-mesenchymal transition in TNBC cells, and correlates with a decrease in MMP2/9 expression

(A) qRT-PCR was used to detect changes in the mRNA expression of EMT-associated genes in PAD1 KD MDA-MB-231 and the control cells. Values are means ± SD. The mRNA for each gene in PAD1 KD cells was normalized to that in shRNA control MDA-MB-231 cells. (B) Western blot was performed to detect changes in the protein expression of EMT-associated genes in PAD1 knockdown or shRNA control MDA-MB-231 cells. (C) Immunofluorescence staining was performed to detect changes in the protein expression of EMT-associated genes in PAD1 knockdown or shRNA control MDA-MB-231 cells. Nuclei were counterstained with DAPI (×40). (D) Immunoblotting was used to detect changes in the protein expression of E-Cadherin (E-CAD) in MDA-MB-468 cells transiently silencing PAD1 (PAD1-siRNA) or control cells. (E) Immunoblotting was used to detect changes in the protein expression of E-CAD in MDA-MB-468 cells after the de novo expression of PAD1. (F and G) PAD1 knockdown or shRNA control MDA-MB-231 cells were analyzed for MMP2/9 mRNA by real-time RT-PCR (F) and for protein expression by immunoblot (G). (H and I) MDA-MB-231 cells were treated with 200 μM Cl-amidine. At indicated time, cells were collected and analyzed for MMP2/9 mRNA expression by real-time RT-PCR (H) and for protein expression by immunoblot (I). *P < 0.05. **P < 0.01.

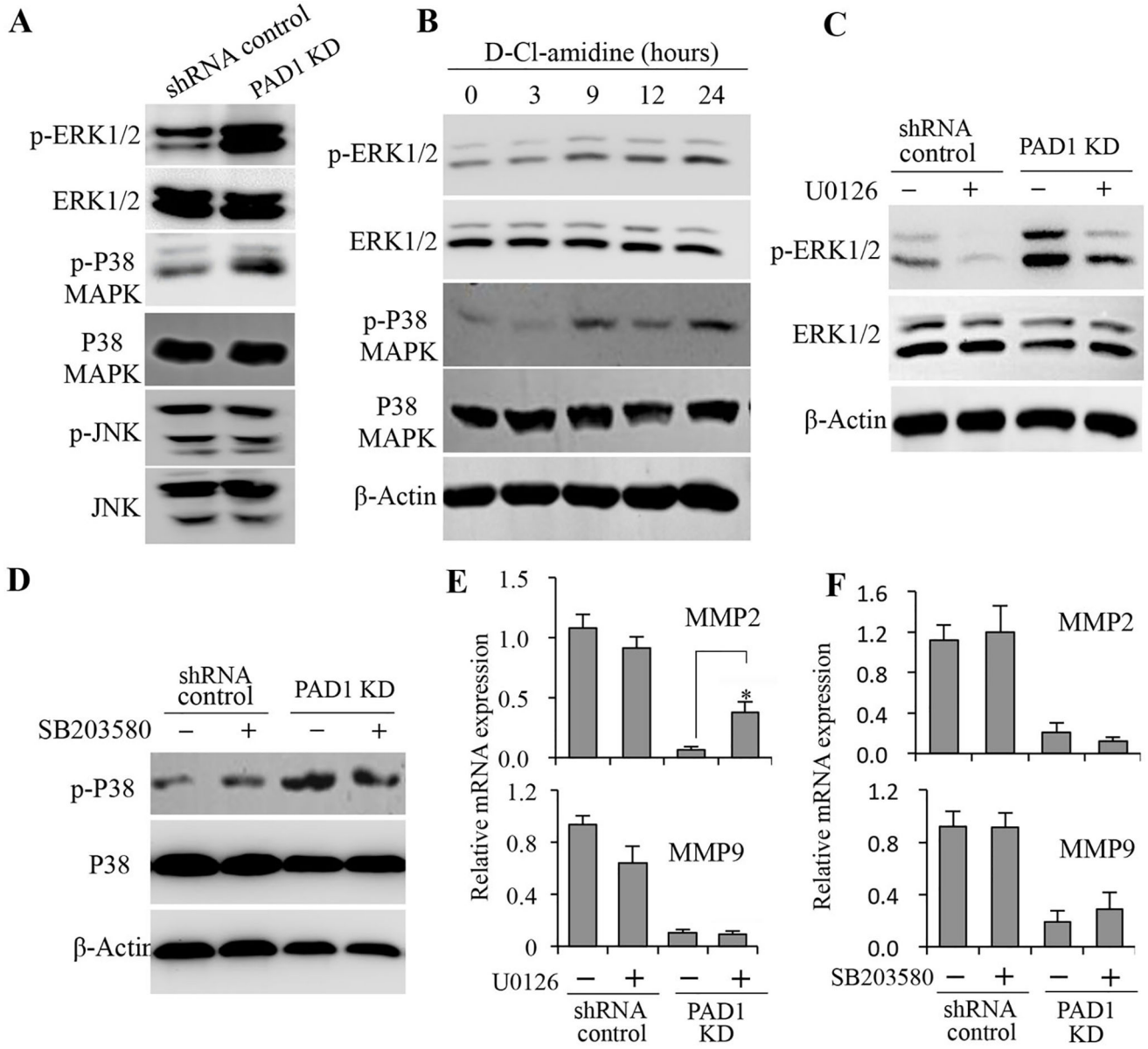

Figure 4. PAD1 represses MMP2 and MMP9 expression through inhibition of MAPK signaling

(A) Western blot analysis of p-ERK1/2, ERK1/2, p-P38, P38, p-JNK, JNK in MDA-MB-231 cells depletion of PAD1 or the shRNA control cells. (B) Western blot analysis of MDA-MB-231 cells treated with D-Cl-amidine using anti-p-ERK1/2, anti-ERK1/2, anti-p-P38 and anti-P38 antibodies. β-Actin served as loading control. (C) Western blot analysis of PAD1-depleted or the control MDA-MB-231 cells treated for 4 hours with 10 μM U0126. Immunoblotting of cell lysates were then performed using anti-p-ERK1/2 and anti-ERK1/2 antibodies. β-Actin served as loading control. (D) Western blot analysis of PAD1-depleted or the control MDA-MB-231 cells treated for 4 hours with 10 μM SB203580. Immunoblotting of cell lysates were then performed using anti-p-P38 and anti-P38 antibodies. β-Actin served as loading control. (E and F) PAD1 knockdown or shRNA control MDAMB231 cells were treated for 4 hours with (E) 10 μM U0126, (F) 10 μM SB203580 and then analyzed for

MMP2 and MMP9 mRNA expression by real-time RT-PCR. All values shown are mean ± SD. *P < 0.05.

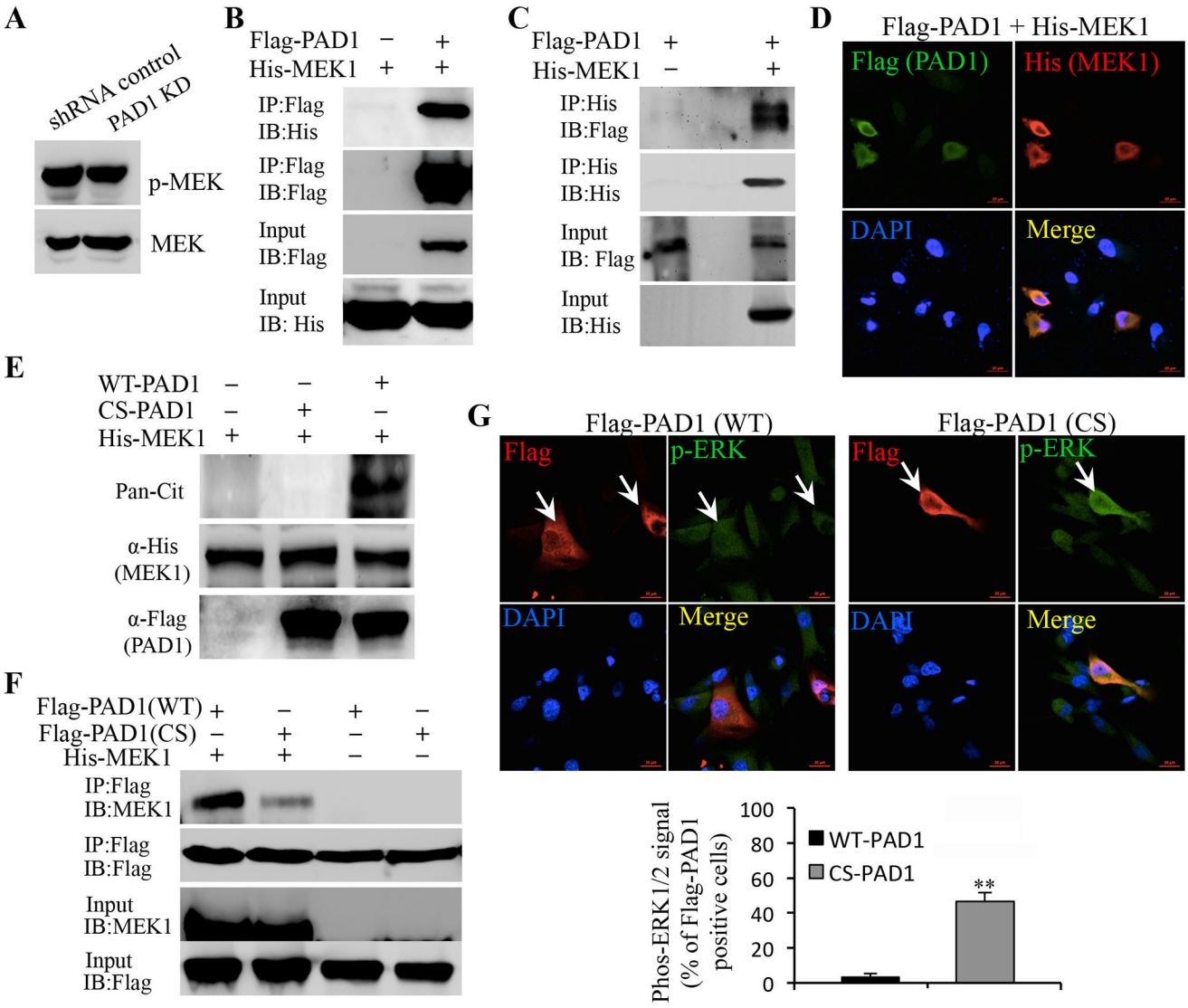

Figure 5. Citullination of MEK1 by PAD1 inhibits MEK-ERK1/2 signaling activation

(A) Western blot showing that the shRNA-mediated depletion of PAD1 in MDA-MB-231 cells did not affect MEK activation versus shRNA control cells. (B and C) Reciprocal co-immunoprecipitation analysis in HEK293 cells revealed that PAD1 interacts with MEK1. (D) Immunofluorescence analysis showing that PAD1 and MEK1 colocalized in the cells. Nuclei were stained with DAPI (scale bar, 20μm). (E) Citrullination of MEK1 by enzymatically active PAD1 *in vitro*. His-tagged MEK1 proteins were treated with either WT or C645S mutant PAD1 (Flag-tagged). The reactions were assessed by western blot using anti-Pan-Cit antibody. His-MEK1 protein without PAD1 treatment was used as a negative control. Anti-His and anti-Flag western blots confirmed equal protein loading. (F) Co-immunoprecipitation analysis showed decreased levels of MEK1 binding to C645S PAD1. Cells transfected with Flag-PAD1 only was used as a negative control. Anti-Flag and anti-MEK1 western blots confirmed equal protein loading. (G) Immunofluorescence analysis showed that C645S PAD1 led to activation of ERK1/2. MDA-MB-231 cells transfected with Flag-PAD1 (WT) or Flag-PAD1 mutant (CS) were stained against the Flag-tag (red) and p-

ERK1/2 (green). Nuclei were stained with DAPI. Signals were quantified (**P < 0.01 PAD1 CS vs. PAD1 WT). Scale bar, 20μm.

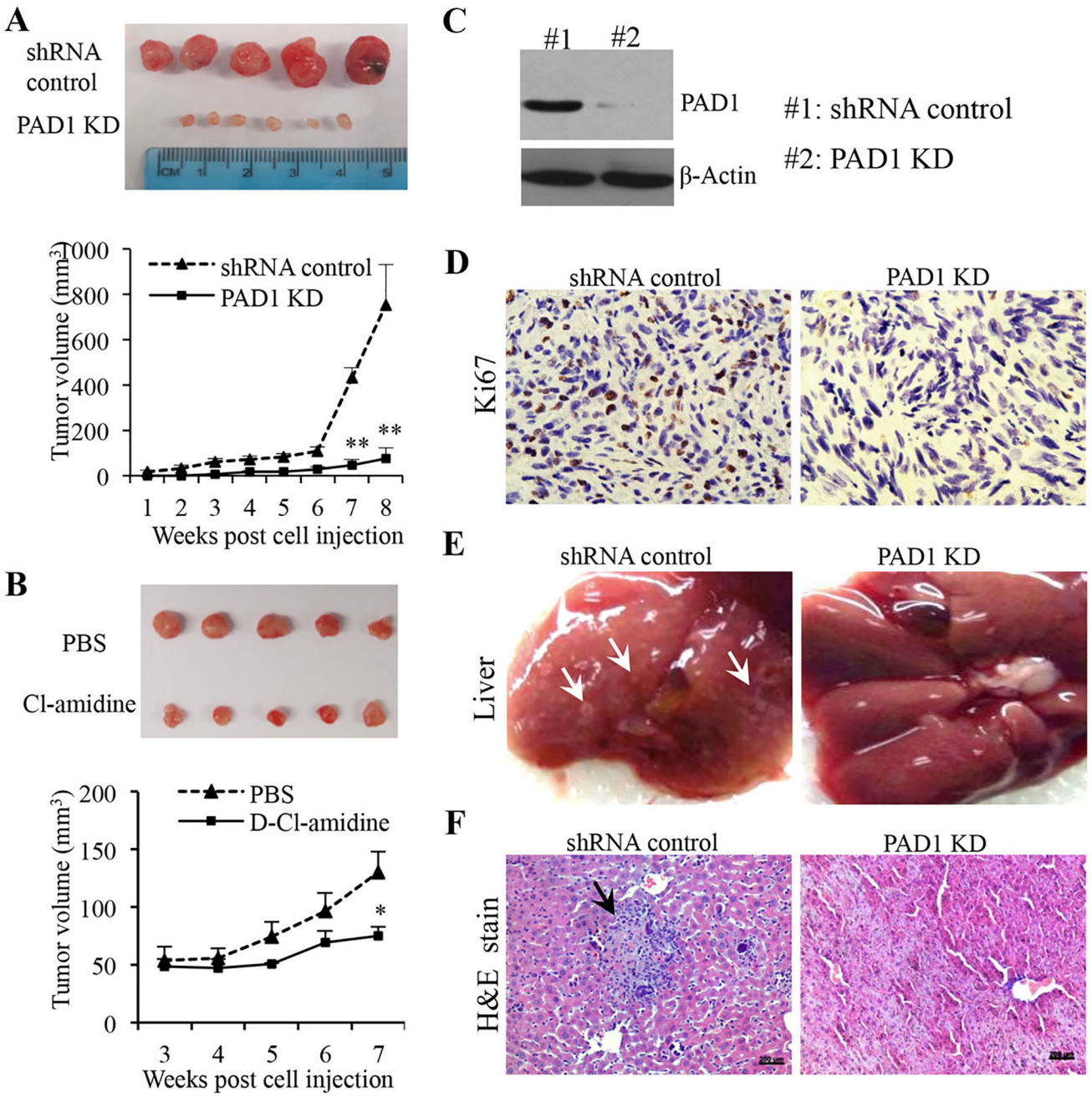

Figure 6. PAD1 depletion or inhibition reduces tumor growth and metastasis of MDA-MB-231 cells in nude mice

(A) The represented tumors formed by PAD1 KD MDA-MB231 cell injection (n=6) or the shRNA control cell injection (n=5) at harvest time. The lower panel shows the volume of tumors at indicated time after cell implantation. The volume of each tumor was quantified, and the average volume was plotted. **P < 0.01. (B) The represented tumors after treatment with D-Cl-amidine or PBS. The lower panel shows growth curves of tumors in nude mice. Data are shown as the mean ± SD. *P < 0.05. (C) Western blotting was performed to confirm the knockdown efficiency of PAD1 in established tumors. β-Actin was used as loading control. (D) Immunohistochemistry staining for Ki67 was performed in PAD1 KD

MDA-MB-231 or control cells using anti-Ki67 antibody (Santa Cruz Biotechnology). Representative micrographs were presented from three independent experiments (40X). (E) Images of metastatic liver nodules spreading throughout the live tissues in mice injected with shRNA control MDA-MB-231cells. PAD1 knockdown clearly abolished the metastasis. Arrows indicate tumor foci. (F) Hematoxylin and eosin (H&E) staining was used to visualize the metastatic nodules in tumors from mice injected with shRNA control MDA-MB-231cells. Arrows indicate tumor foci. Scale bar = 200 μm.